

An Experimental Apparatus for Observing Deterministic Structure Formation in Plate-on-Pedestal Ice Crystal Growth

Kenneth G. Libbrecht

Department of Physics, California Institute of Technology
Pasadena, California 91125

Abstract. We describe an experimental apparatus for making detailed morphological observations of the growth of isolated plate-like ice crystals from water vapor. Each crystal develops a plate-on-pedestal (POP) geometry, in which a large, thin, plate-like crystal grows out from the top edge of an initially prismatic seed crystal resting on a substrate. With the POP geometry, the substrate is not in contact with the growing plate (except at its center), so substrate interactions do not adversely affect the crystal growth. By controlling the temperature and supersaturation around the crystal, we can manipulate the resulting ice growth behavior in predictable ways, producing morphologies spanning the full range from simple faceted hexagonal plates to complex dendritic structures. We believe that the experimental apparatus described here will allow unprecedented investigations of ice crystal growth behaviors under controlled conditions, identifying and exploring robust morphological features in detail. Such investigations will provide valuable observational inputs for developing numerical modeling techniques that can accurately reproduce the faceted and branched structures that frequently emerge during diffusion-limited crystal growth.

1 Introduction

The growth of crystalline ice Ih from water vapor near the triple point has long been a fascinating case study for understanding the physical processes governing crystal growth (for a review, see [1]). The emerging growth morphologies are largely deterministic, yet highly variable with changing temperature and supersaturation around the crystal. In the pure system of ice and water vapor (with no background gas), measured growth rates as a function of temperature, supersaturation, and facet surface are controlled mainly by attachment kinetics at the ice surface. Quantitative measurements thus provide insights into the structure of the ice surface, including surface premelting and step energies on facet surfaces, which are both poorly understood at present [2]. In the presence of an inert background gas, particle transport also plays an important role, and the ice system can be used for quantitative investigations of the diffusion-limited growth of structures that are both branched and faceted [3, 4, 5, 6]. Recent measurements suggest that structure-dependent attachment kinetics (SDAK) is also a key factor determining the observed ice growth behavior [7, 8].

Ukichiro Nakaya pioneered the study of ice crystal growth from water vapor in the 1930s, producing isolated crystals on rabbit hair [9]. Numerous researchers have subsequently grown ice crystals on various thin fibers, on capillary tubes, on various substrates, and even on the ends of electrically enhanced ice needles (see [1] and references therein). Each experimental method has its own merits for making quantitative growth measurements as well as qualitative morphology observations that reveal different aspects of ice growth behavior.

We recently described the formation of “plate-on-pedestal” (POP) ice crystal growth, in which a

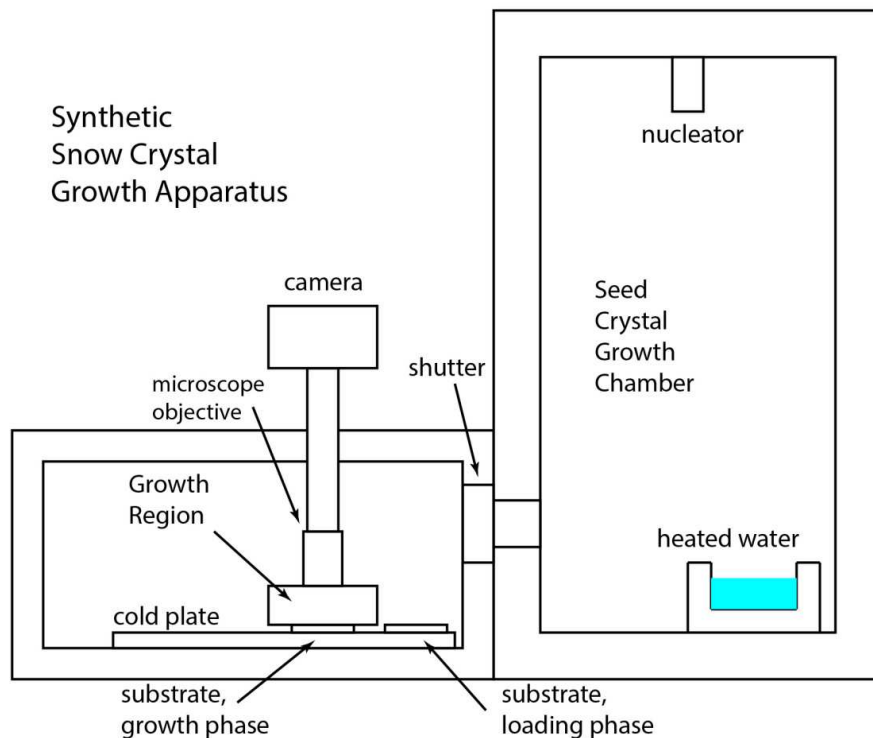


Figure 1: A schematic diagram of our apparatus for growing and photographing synthetic snow crystals, described in detail in the text.

thin plate-like crystal grows out from a small prismatic seed crystal resting on a substrate. Notably, the growing ice plate forms entirely above the substrate, being held up only by a small ice pedestal. As described in [8], this unusual structure is especially useful for exploring the SDAK instability, although growth on ice needles shows perhaps even greater promise in this regard [5, 10].

To our knowledge, the POP method for growing ice crystals was first described by Gonda, Nakahara, and Sei in the 1990s [11, 12], although the authors did not explicitly point out the POP structure of their ice crystals. It appears that little subsequent work has been done to further develop the POP method. The present paper picks up where these earlier works left off, seeking to develop some of the unrealized potential of the plate-on-pedestal method.

Beyond its application in scientific investigations of crystal growth dynamics, the POP method also presents considerable opportunity to further the art of ice crystal growth from water vapor. In that direction we have been exploring various techniques to grow ice crystals that resemble atmospheric snow crystals, exhibiting a broad variety of branched and faceted structures with their distinctive six-fold symmetry. Time-lapse photography of the POP crystals also reveals many aspects of snow-crystal growth behavior with unprecedented clarity.

2 Experimental Apparatus

Figure 1 shows an overview of the hardware we use for growing ice crystals from water vapor in a background gas of air. During a typical run, freely floating seed crystals are generated continuously in the seed crystal growth chamber (see Figure 1), as described below. To produce a growing POP crystal, a shutter is opened to allow some of the seed crystals to fall randomly onto the substrate in its loading position. The substrate is then moved to the growth region, where it is positioned to place an isolated seed crystal at the center of the microscope field of view. Moist air is then blown gently onto the substrate, causing the test crystal to grow. The temperature and supersaturation around the crystal can be changed as it grows, while a camera records its development. We now examine the various parts of this apparatus in detail.

2.1 The Seed Crystal Growth Chamber

Seed crystals are produced in a custom-built cold chamber with inside dimensions of approximately 40x40x100 cm, the large dimension being the height. The chamber is cooled by a laboratory chiller (SP Scientific/FTS RS33-LT) that circulates temperature-regulated coolant (methanol) through the walls of the chamber as well as the adjoining cold plate (see Figure 1). Ordinary laboratory air fills the seed chamber, which does not have an air-tight seal. The chamber is insulated with approximately 5 cm of styrofoam sheeting covering all the outer surfaces.

An insulated container containing one liter of ordinary tap water rests on the bottom of the seed chamber, as shown in Figure 1, and the water temperature is kept constant by a temperature regulator using an immersed water heating element and water temperature sensor. The top of the container is open to the air, so water evaporates and is carried by convection to the rest of the chamber. As we have described previously [13, 14], convective mixing of the air produces a fairly uniform temperature and supersaturation within the seed chamber, except immediately above the water reservoir and near the chamber walls (which soon become covered with frost, lowering the nearby supersaturation). Water vapor is continually removed from the air by growing ice crystals and by frost depositing on the walls of the chamber, and this water vapor is continually replenished by evaporation from the water reservoir. The air temperature is easily measured by placing a thermistor inside the chamber. The supersaturation is more difficult to determine, but can be inferred by the morphology of the growing crystals. We therefore adjust the water temperature and chiller temperature until the desired chamber air temperature and seed crystal morphology are produced.

We typically set the chiller temperature to -19 C and the water temperature to 17 C, as this yields a continuous supply of thin, hexagonal plate-like seed crystals with diameters in the 20-50 micron range. The air temperature inside the seed crystal growth chamber remains near -15 C. Higher water temperatures (while maintaining the air temperature near -15 C) yield higher supersaturations and more dendritic structures. Thicker plates can be produced with different air temperatures, while temperatures near -5 C yield columnar crystals. See [13, 14] for additional details on free-fall growth chambers and the crystal morphologies that result.

The nucleator at the top of the chamber consists of a small stainless steel chamber (a standard 1.33-inch conflat nipple) with an interior volume of ~ 25 cm³ that is connected to a solenoid valve. The nucleator assembly is inside the growth chamber, so its temperature is approximately -15 C during operation. Pressurized room air flows into the nucleator through a constriction that limits the flow. The flow rate is slow enough that the air temperature becomes roughly equilibrated inside

the nucleator. Likewise, frost condenses on the inner walls of the nucleator, so the water vapor content of the air is near the saturated value. Every ten seconds the solenoid valve is opened, causing the pressurized air to rapidly expand and enter the growth chamber. The rapid expansion produces a small amount of air that is sufficiently cooled to nucleate ice crystals. Air pressures as low as 15 psi will nucleate crystals, and we usually operate with 30 psi. Water buildup inside the nucleator is removed after each run by operating it for several hours when the chamber is at room temperature. With no initial ice buildup, the nucleator can run continuously for at least ten hours without difficulty.

The nucleated crystals float freely as they grow, until they eventually settle to the bottom of the chamber. The fall times are typically a few minutes, depending on temperature and supersaturation. Pulsing the nucleator valve open every ten seconds thus produces a steady-state in which roughly a million seed crystals are growing inside the chamber at any given time (this number being determined by a visual estimate of the typical spacing between crystals floating inside the chamber during operation). Shining a bright flashlight into the chamber reveals sparkles caused by reflections off the crystal facets, and this is a convenient way to verify that seed crystals are present.

Compressed air for both the nucleator and the crystal growth region is supplied by an ordinary workshop air compressor with a built-in storage tank and regulator, which automatically maintains the required 30 psi air pressure. The compressed air is passed through an oil filter, then an activated charcoal filter (containing coconut charcoal) to remove remaining chemical contaminants from the air, and then a fine-pore fiber filter to remove any remaining charcoal dust.

An aperture in the side of the seed crystal growth chamber connects it to the adjoining main growth chamber (the left side of Figure 1). The cold plate within the main chamber is cooled using the same circulating coolant that flows through the walls of the seed chamber. To grow an POP crystal, the substrate is first moved into its loading position (see Figure 1) and a shutter is opened between the two chambers. Random air flow between the chambers carries a small number of crystals into the second chamber, and some of these fall onto the substrate, a process that takes a few seconds. The substrate is then moved to a covered region within the main growth chamber, and a suitably isolated seed crystal is centered under the microscope for subsequent growth and observation.

2.2 The Growth Chamber

Figure 2 shows a more detailed view of the growth region shown in Figure 1. The substrate is an uncoated sapphire disk, 50.8 mm in diameter and 1 mm thick, with the sapphire c-axis perpendicular to the disk surface. The principal advantages to using sapphire in this application are its high thermal conductivity and resistance to scratching. The substrate slides on an anodized aluminum plate with a temperature T_1 maintained by a temperature controller (Arroyo Instruments model 5310) using a thermistor temperature sensor (Cole-Parmer Digi-Sense 08491-15) in the aluminum plate and thermoelectric heating/cooling modules beneath it. The thermistors have an absolute accuracy better than ± 0.1 C, and the temperature regulation is stable to better than ± 0.01 C under normal operation. However, the temperature of the substrate and especially the air immediately above it are not precisely equal to the aluminum plate temperature, and this adds uncertainty to the ice crystal growth temperature.

The heat exchanger above the substrate is an aluminum plate at a temperature T_2 maintained by a separate temperature controller. Filtered room air from the air compressor first passes through a baffled pre-cooler kept near $T_{precool} = 0$ C ($T_{precool} > T_2$) to partially cool the air, and to remove

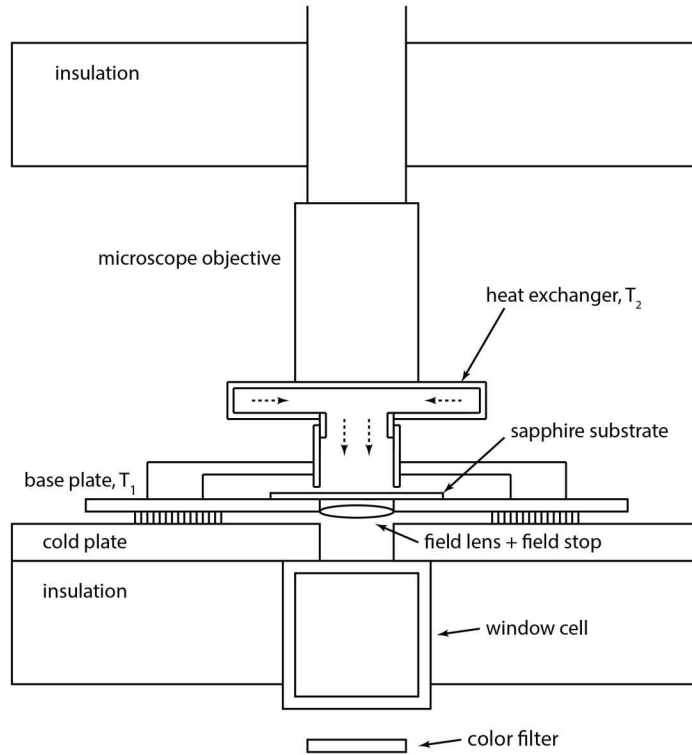


Figure 2: A schematic diagram of the growth region shown in Figure 1. Once a test crystal has been positioned at the center of the microscope field-of-view, moist air passing through the heat exchanger is blown onto the substrate, causing the crystal to grow. The base-plate temperature T_1 , the heat-exchanger temperature T_2 , and the air flow rate through the heat exchanger can all be controlled as the crystal growth is observed.

a large fraction of the water vapor initially present in the air. The air then passes through a series of serpentine channels in the heat exchanger plate before blowing down onto the substrate and the growing ice crystal. The air flow rate is typically 200-300 ccm, measured using a tapered-tube flow meter and controlled with a simple needle valve. This flow rate replaces air in the guide tube (between the heat exchanger and the substrate, as shown in Figure 2) about once per second. The interior diameter of the guide tube is 1.6 cm, and its overall length (from the bottom of the heat exchanger to the substrate) is approximately 2.3 cm. Air flows into the guide tube via four channels in the heat-exchanger plate, arranged symmetrically around the circumference of the top of the guide tube. The equal flow rates through the four input channels, along with the cylindrical geometry of the guide tube assembly, were engineered to produce a nearly cylindrically symmetric downward flow pattern within the guide tube, with the flow axis centered on the growing crystal. The guide tube temperature is kept near the substrate temperature T_1 , and the guide tube is thermally isolated from the heat exchanger by a thin-walled plastic tube.

During the initial cooldown of the apparatus, air is passed through the heat exchanger for 30 minutes to deposit ice on its inner surfaces. The temperature is set to $T_2 < -20$ C during this time to make sure ice (and not supercooled water) is deposited inside the heat exchanger. Once the heat exchanger has been preconditioned in this way, air passing through it will exit at temperature T_2 and be saturated with water vapor relative to ice at T_2 . As it approaches the substrate, the air cools to near $T_1 < T_2$ and thus becomes supersaturated. The degree of supersaturation is controlled by setting the temperature difference $\Delta T = T_2 - T_1$ as well as the air flow rate. To lowest order, the supersaturation is proportional to ΔT^2 [1]. If the supersaturation is sufficiently high, water droplets will condense on the substrate around the growing ice crystal. In general, a higher ΔT and a higher flow rate produce a higher supersaturation around the growing ice crystal.

Modeling the temperature and supersaturation at the growing ice surface is problematic with this apparatus for a number of reasons. The Reynolds number of the flow is approximately 10, so the flow is probably not perfectly laminar, and the timescale for the air in the guide tube to become equilibrated via diffusion with the guide-tube walls is comparable to the time it takes air to flow through the tube. Moreover, a stagnation point in the flow occurs where the flow axis of the system intercepts the substrate surface, at the position of the growing crystal, further complicating the flow and thermal analysis. More importantly, water droplets condensing on the substrate near the crystal substantially alter the supersaturation field, and the amount of water condensation changes dramatically with changes in ΔT and flow rate. The thermal connection between the edge of a growing POP crystal and the substrate below is also a bit difficult to determine accurately. For all these reasons, we do not expect that the apparatus described here will be well suited for performing precision measurements of ice growth rates under known conditions. It is better suited for more qualitative studies examining ice crystal morphologies and growth behaviors.

The microscope objective shown in Figure 2 is part of the heat exchanger assembly, but it is kept a few degrees warmer than T_2 using a heater dissipating 1-2 Watts into the objective body. This elevated temperature is necessary to keep fog from condensing on the glass face of the objective, which would interfere with optical imaging. We typically use a Mitutoyo 5X Plan Apo objective with an achromatic reimaging lens (focal length 250 mm) immediately behind it. This objective has a working distance of 34 mm, a numerical aperture of 0.14, resolution of $2 \mu\text{m}$, and a depth-of-field of $14 \mu\text{m}$. Focusing is done by moving the camera body (on a StacShot rail), and some amount of focus stacking is typically needed for optimal imaging of large crystals, owing to the shallow depth-of-field. The image projects to about $1 \mu\text{m}$ per pixel of the sensor on our Canon EOS 5D camera.

The field lens shown in Figure 2 reimages a color filter onto the pupil of the objective for achieving Rheinberg illumination. With this technique, the background in the image plane remains uniform regardless of the color filter used. Our filters are not monochromatic, but have a variety of color patterns. With the Rheinberg optical set-up, the color filter provides different colors of light illuminating the crystal at different input angles, while all colors illuminate the image plane uniformly. The transmitted light is refracted through the crystal, which acts as a complex lens. The birefringence and color dispersion of the ice are both negligible in this optical arrangement. Using Rheinberg illumination adds a sense of depth to the photographs, which helps accentuate the internal structure and surface patterning of the growing ice crystals. The window cell provides thermal insulation between the room and the cold plate. A variety of baffles and constrictions (not shown in Figure 2) prevent condensation on the different optical components while maintaining the desired temperature profiles during operation.

It should be emphasized that producing an isolated seed crystal on the substrate is perhaps the most difficult step in using this apparatus. In contrast, the growth process itself is quite straight-

forward. Seed crystals fall randomly during loading, and their surface density on the substrate is adjusted by how long the shutter remains open with the substrate in the loading position. Also, many seed crystals are malformed and are therefore not suitable candidates for further growth. If the surface density of seed crystals is too low, it may not be possible to locate a well formed specimen. If the density is too high, then it may not be possible to obtain a sufficiently isolated crystal. Often several tries are needed to find a suitable seed crystal, taking anywhere from 1-30 minutes. Between tries, the substrate is heated to evaporate away the existing crystals.

We often use a heating trick to load larger and better formed seed crystals. After warming the substrate to clean it, we set the substrate temperature controller to the desired loading temperature T_1 , but then begin the loading process while the substrate temperature is still higher than T_1 . With proper timing, the warmer substrate tends to evaporate away smaller crystals, while larger ones survive just long enough for the substrate temperature to reach T_1 , and at that point the remaining crystals are stable. The end result is that smaller crystals are removed, leaving only larger seed crystals behind.

When growing large, plate-like ice crystals, the ideal seed crystal is a well-formed hexagonal plate with its basal surfaces parallel to the substrate, and with no other crystals closer than at least 5 mm on the substrate. The subsequent growth phase typically lasts 30-90 minutes and can be recorded via the imaging system. The temperatures T_1 and T_2 are adjusted with time (it requires about a minute for each to stabilize), along with the flow rate, to obtain the desired growth behaviors. At the end of the growth phase, the substrate is heated to just below 0 C so that the ice crystals evaporate away, at which point the process can be started once again. After a typical day-long run growing crystals, the entire system is warmed to room temperature and baked to remove water.

Because a growing crystal is surrounded by air that has passed through the heat exchanger, we took special care to reduce chemical contaminants in that air. The charcoal filter was put into the air stream to remove contaminants, and the fiber filter downstream from the charcoal filter was tested for odor emission. The heat exchanger is baked at 40 C overnight before each run to remove residual contaminants. We have not made quantitative measurements of the remaining contaminant level, but we are able to grow quite thin ice plates near -15 C. This observation is itself a good indication that the air flowing into the growth region is sufficiently clean, since contaminants are known to inhibit thin plate growth at this temperature [15].

3 Investigations of Growing Crystals

To date we have confined our crystal-growth investigations to temperatures between -5 C and -20 C, mostly growing large, thin, plate-like crystals with an overall plate-on-pedestal (POP) structure. It should be possible to grow other morphologies using this same apparatus, but our current system only allows imaging from the top, which is best suited for observing plate-like crystals.

3.1 Hexagonal Plates

Figure 3 demonstrates several morphological features we often see when growing hexagonal plate-like crystals. Focusing on the first crystal in Figure 3, it was grown with $T_1 = -15$ C and $T_2 = -14$ C, so the ice temperature was near -15 C and the supersaturation was below the water saturation level. The small star-shaped figure at the center of the crystal outlines the pedestal that supports the POP growth. The pedestal is approximately 70 μm in diameter, only slightly larger than the

diameter of the initial seed crystal. At sufficiently low supersaturations, the seed crystal will grow out while the edge remains in contact with the substrate. At temperatures within several degrees of -15 C, however, even modest supersaturations yield the POP morphology. All POP crystals thus have a small central pedestal, although it is not always obvious in the photographs.

Note that six radial “ridges” are clearly visible in the first crystal in Figure 3, dividing the hexagon into six sectors. Similar ridges are present in many POP crystals growing near -15 C, and they are commonly seen in natural snow crystals as well. The ridges originate at the corners of the hexagon and thus trace the location of the corners as a function of time as the crystal grew. For perfectly symmetrical growth, the ridges would all be straight. The growth was not perfectly symmetrical with this crystal, so some of the ridges are slightly curved. The origin of the asymmetry was some combination of neighboring crystals (which affect the supersaturation in the air surrounding the observed crystal), air flow asymmetries, and seed crystal asymmetries (for example, tilt of the basal surfaces relative to the substrate). The largest asymmetry is typically from neighboring crystals; in the absence of neighbors, we can often grow crystals that are more symmetrical than the first example in Figure 3.

The concentric hexagonal “ribs” seen in both crystals in Figure 3 arise when the growth conditions are altered with time. The ribs are essentially like tree rings that record changes in the growth of the edge of the crystal as a function of time. With constant external conditions, these ribs are largely absent. Whenever the growth conditions are changing, however, ribs like those shown in these examples are common morphological features.

The faint circular features seen in the first crystal Figure 3 are inwardly growing macrosteps on the top surface of the plate. These are best imaged using Rheinberg illumination, which highlights such features. We have observed that the top surfaces of many POP crystals are typically quite flat except for similar macrosteps. The ribs and ridges are usually surface features confined to the lower surfaces of POP crystals (the surface closer to the substrate). One goal of future 3-D computer modeling efforts will be to reproduce these specific morphological features in hexagonal POP crystals, as they are observed over a broad range of conditions.

The first crystal in Figure 3 also exhibits four curved lines that arise from dislocations in the ice crystal. These lines are unusual, suggesting that most simple plates are essentially dislocation free. This particular crystal was allowed to branch (forming six separate branches) early in its growth, and the branches later merged back together to form a single plate. The dislocations appeared during these mergers, as the branches did not recombine with atomic accuracy. Without the branching step, plates typically do not exhibit dislocation lines.

We have been able to grow hexagonal plates up to 2 mm in diameter rather easily. The radius increases typically as $R \sim t^\alpha$, where t is the growth time and α is between 0.6 and 0.7, depending on initial conditions and other factors. Figure 4 shows some typical growth rate data. Hexagonal plates grow quite readily at temperatures between -17 C and -13 C.

In [8] we presented a quantitative analysis of growing hexagonal plates, using cellular automata modeling to extract information about the attachment kinetics on the prism surface. Those measurements indicated the importance of the SDAK instability in the growth of plate-like ice crystals. The work described in the present paper supports that conclusion, but we have not done additional quantitative investigations of the growing crystals, focusing instead on morphological investigations and on techniques for growing stellar snow crystals similar to those found in the atmosphere.

Going beyond simple hexagonal plates, Figure 5 shows a more elaborate sectored-plate snow crystal made in this apparatus, which exhibits many of the same morphological features seen in hexagonal plates. Ridges, ribs, macrosteps, and faceted prism surfaces are all present in this photo-

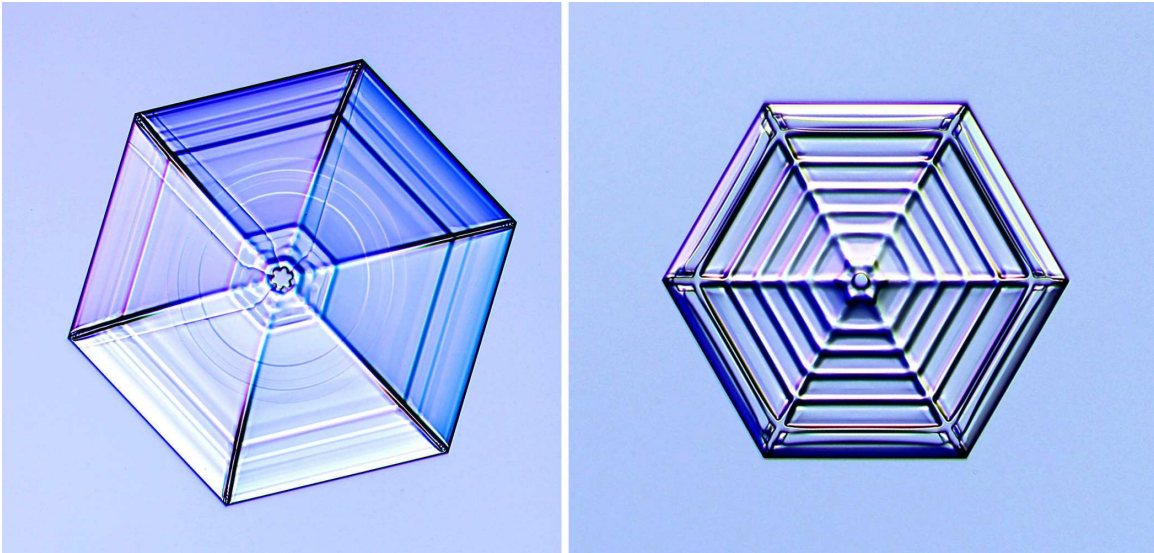


Figure 3: Photographs showing two hexagonal POP ice crystals with several commonly seen morphological features that are described in detail in the text. The crystal on the left exhibits 1) radial “ridges” that divide the plate into six sectors; 2) several concentric hexagonal “ribs”; 3) several concentric circular macrosteps that grow slowly inward; and 4) four curved dislocation lines (two of which flank the upper left ridge). This crystal measures 1.5 mm from tip to tip. The crystal on the right was subjected to periodic temperature changes that yielded a spider’s-web pattern of ridges and ribs. This crystal measures 0.75 mm from tip to tip.

graph, as they are to varying degrees in many of our POP crystals. By examining these features in detail as a function of the applied growth conditions, and by recording their formation and development as a function of time, much can be done to further refine and develop computational methods for simulating diffusion-limited crystal growth.

3.2 Branching

As is well known from numerous previous studies, branching via the Mullins-Sekerka instability is important in snow crystal growth [1], and an example of the branching instability in a POP crystal is shown in Figure 6. The first image in this figure shows a hexagonal plate crystal while it was growing stably, maintaining its overall hexagonal shape as it grew. Increasing ΔT , and thus the supersaturation surrounding the crystal, initiated a branching event. Since the tips of the hexagon projected farther out into the supersaturated air, they accumulated more water vapor and grew more rapidly than other areas on the crystal, causing the tips to project out even farther. The resulting growth instability caused branches to sprout from the corners of the crystal, as demonstrated in Figure 6. Branching events such as these are easily initiated and often observed in our POP crystals.

Increasing the supersaturation to initiate branching in POP crystals often results in the condensation of water droplets on the substrate surface, as shown in two examples in Figure 7. These droplets can remain liquid for hours at temperatures near -15 C, and they prevent the super-

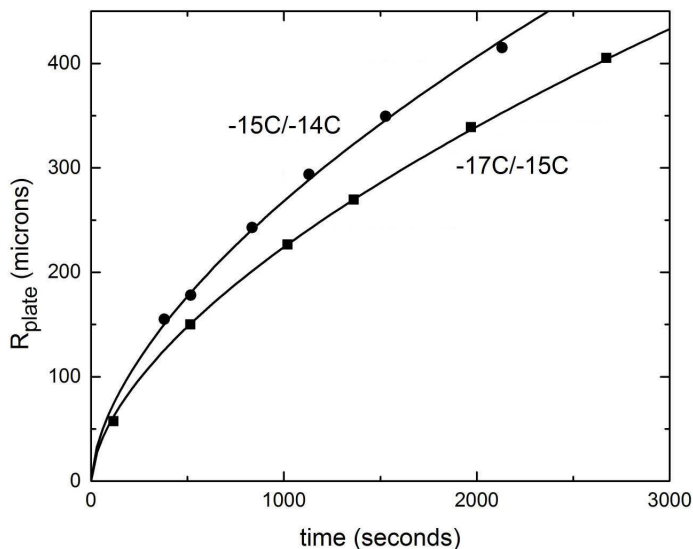


Figure 4: Example measurements of the growth of two hexagonal-plate POP crystals. The plate radius is taken to be half the tip-to-tip distance between opposite corners of each crystal. The curves passing through the data points have the functional form $R = At^{0.6}$. The labels indicate the temperature of the substrate T_1 (first number) and the temperature of the heat exchanger T_2 (second number), which remained constant as the crystals grew.

saturation around the crystal (with respect to ice) from increasing substantially above the water saturation point. Increasing the air flow rate especially tends to cause droplet formation close to the growing crystal. These droplets can be removed by reducing ΔT until they evaporate away, but often they remain surrounding a growing crystal for long periods. In some instances, they appear to stabilize the crystal growth and improve the overall six-fold symmetry of the crystal. Often a neighboring crystal (several millimeters away from the main POP crystal) will grow in such a way that it intersects the substrate as it grows, eventually bringing it into contact with some of the deposited droplets, causing them to freeze. The frozen droplets soon contact neighboring droplets, and the front of frozen droplets expands until the entire field is frozen, a process that typically takes a few minutes. Once the central POP crystal is surrounded by a field of frozen droplets, the supersaturation becomes quite low, inhibiting subsequent growth.

Figure 8 shows an example of what we call an *induced sidebranching event*. By first lowering the supersaturation to produce faceting, and then increasing the supersaturation to stimulate branching, it becomes possible to place sidebranches on a growing crystal in a prescribed way. Figure 9 shows another example where sidebranches were placed five times at approximately uniform intervals along the main branches.

At still higher supersaturations, we might expect to see sidebranches appearing spontaneously with irregular spacing along dendritic branches growing near -15 C, as this is known to occur in diffusion-chamber studies and in natural snow crystals. In the apparatus described here, however, we

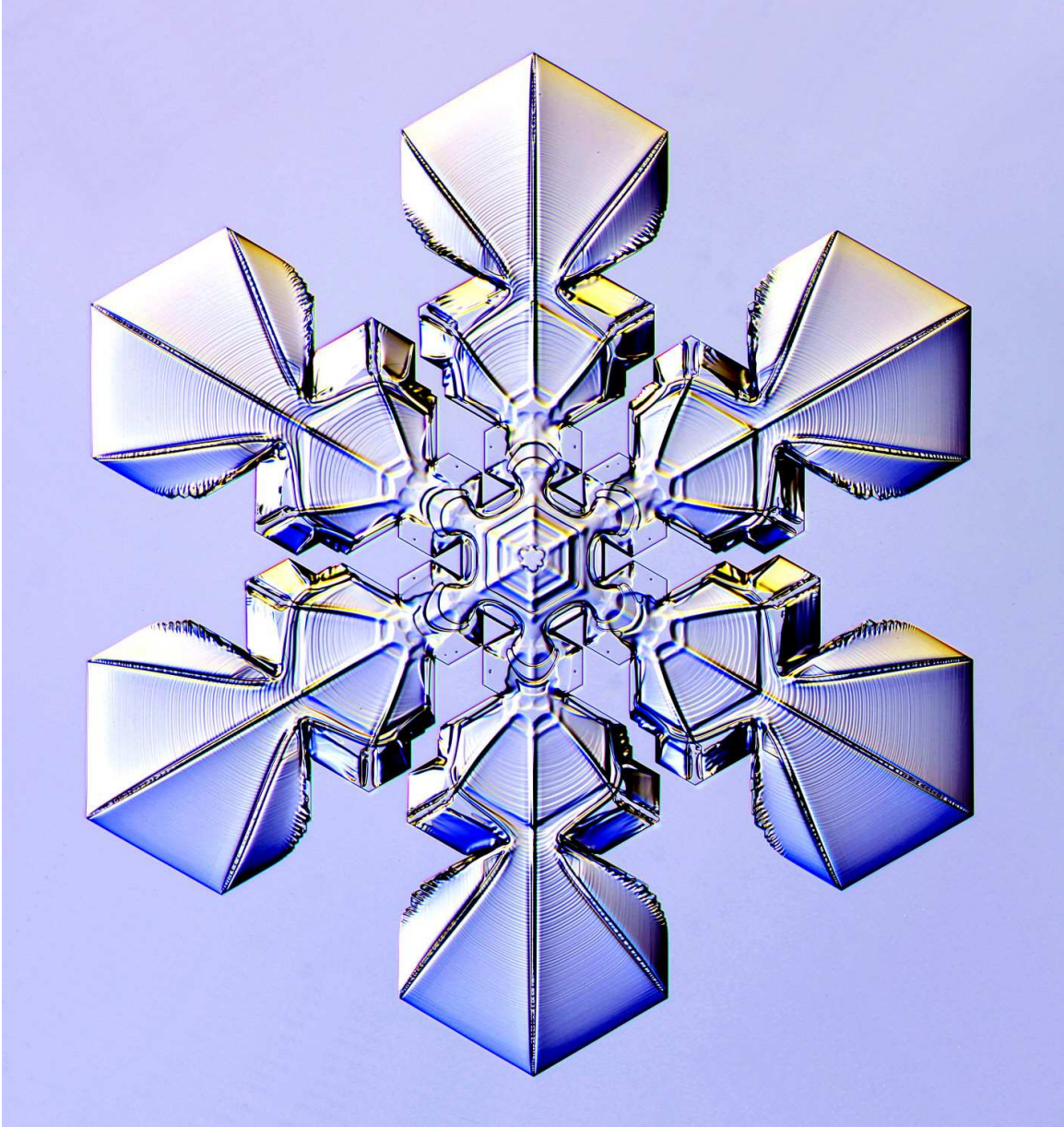


Figure 5: Photograph of a large POP crystal that resembles sectored-plate snow crystals that grow in the atmosphere. The size of this crystal is 3.3 mm from tip to tip. A variety of ridges, ribs, and macrosteps are all visible in the photograph. The irregularly shaped nub in the center of the crystal outlines the small pedestal that supports the much larger plate above the substrate.

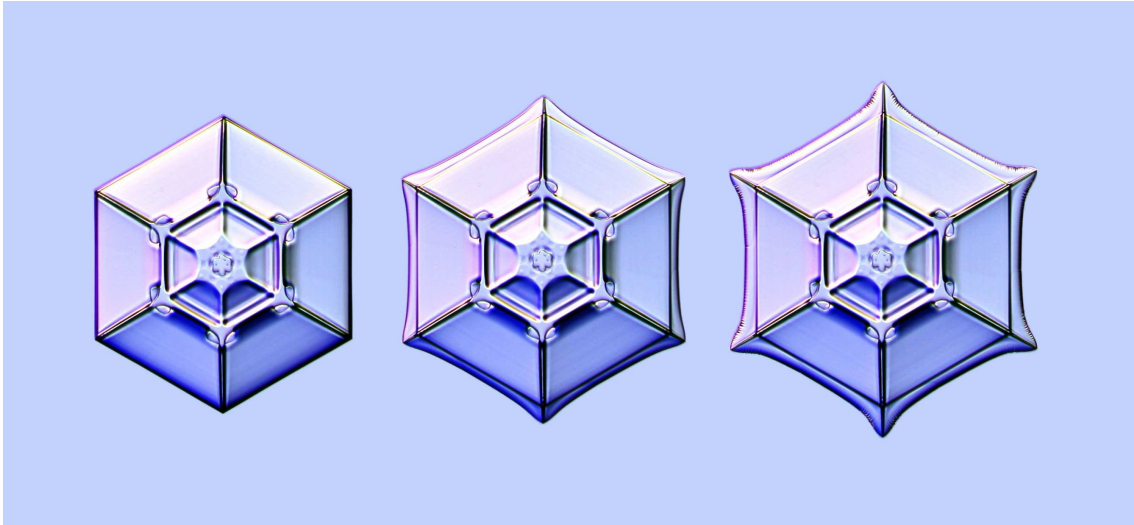


Figure 6: A series of photographs, taken at different times, showing the formation of branches on a hexagonal POP crystal. The crystal measured 0.6 mm from tip to tip in the first photograph, when it was growing stably with $T_1 = -13$ C and $T_2 = -12$ C. Reducing T_1 to -15 C increased the supersaturation around the crystal, initiating the development of branches as the corners of the hexagonal plate.

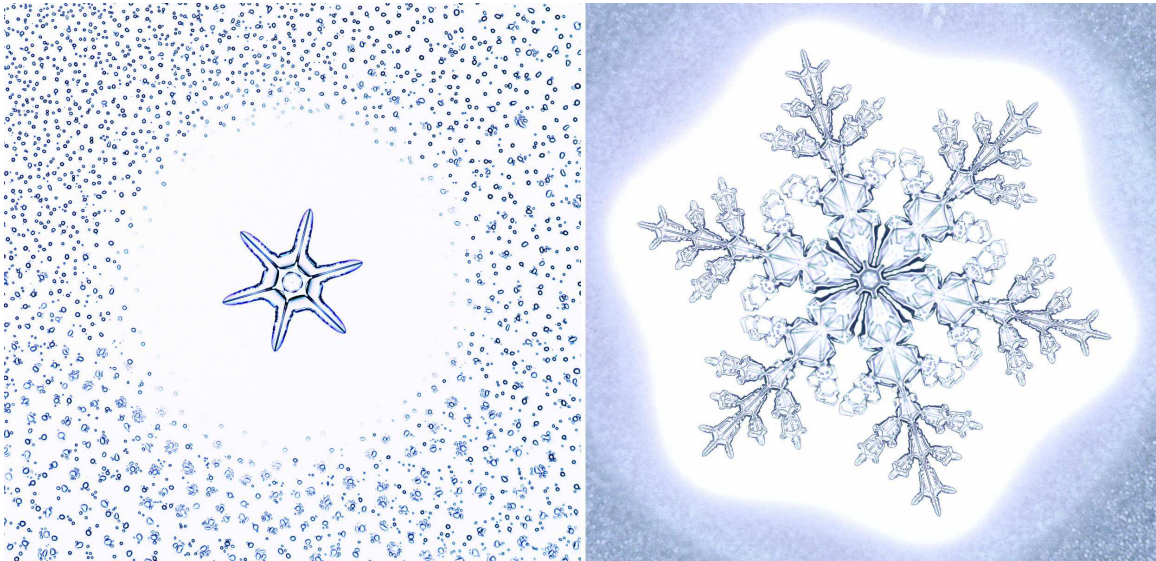


Figure 7: Two photographs of POP crystals showing the deposition of water droplets on the substrate surrounding each crystal. The crystals measured 0.36 mm (left) and 1.9 mm (right) from tip to tip. Increasing either ΔT or the air flow rate generally results in droplet deposition closer to the growing crystals.

have not found it possible to achieve sufficiently high supersaturations for spontaneous sidebranching, because of the formation of water droplets on the substrate.

4 Discussion

At present, our understanding of the diffusion-limited growth of structures that are both branched and faceted remains quite poor. The cellular automata method for numerical modeling of such structures holds much promise [3, 4, 5, 6], but we have not yet learned what input physics should be applied in those models. We believe that structure-dependent attachment kinetics (SDAK) is a key element to be included [7, 8], but many aspects of the SDAK hypothesis remain untested. Detailed morphological comparisons between computational models and ice growth experiments will likely play an important role in the development of those models, especially in three dimensions. To this end, ice crystals grown in the apparatus presented above should provide many useful insights toward a better understanding of ice growth behavior in particular, and of diffusion-limited crystal growth more generally.

References

- [1] K. G. Libbrecht. The physics of snow crystals. *Rep. Prog. Phys.*, 68:855–895, 2005.
- [2] Kenneth G. Libbrecht and Mark E. Rickerby. Measurements of surface attachment kinetics for faceted ice crystal growth. *J. Crystal Growth*, (377):1–8, 2013.
- [3] C. A. Reiter. A local cellular model for snow crystal growth. *Chaos, Solitons, and Fractals*, 23:1111–1119, 2005.
- [4] Janko Gravner and David Griffeath. Modeling snow-crystal growth: A three-dimensional mesoscopic approach. *Phys. Rev. E*, 79:011601, Jan 2009.
- [5] Kenneth G. Libbrecht. Quantitative modeling of faceted ice crystal growth from water vapor using cellular automata. *J. Computational Methods in Phys.*, (ID-174806), 2013.
- [6] James G. Kelly and Everett C. Boyer. Physical improvements to a mesoscopic cellular automaton model for three-dimensional snow crystal growth. *arXiv*, (1308.4910), 2013.
- [7] K. G. Libbrecht. Explaining the formation of thin ice-crystal plates with structure-dependent attachment kinetics. *J. Cryst. Growth*, 258:168–175, 2003.
- [8] K. G. Libbrecht. An edge-enhancing crystal growth instability caused by structure-dependent attachment kinetics. *arXiv*, (1209.4932), 2012.
- [9] U. Nakaya. *Snow Crystals*. Harvard University Press: Cambridge, 1954.
- [10] Kenneth G. Libbrecht. A dual diffusion chamber for observing ice crystal growth on c-axis ice needles. *arXiv*, (1405.1053), 2014.
- [11] S. Nakahara T. Gonda and T. Sei. The formation of side branches of dendritic ice crystals growing from vapor and solution. *J. Cryst. Growth*, 90:183–187, 1990.

- [12] T. Gonda and S. Nakahara. Dendritic ice crystals with faceted tip growing from the vapor phase. *J. Cryst. Growth*, 173:189–193, 1997.
- [13] Kenneth G. Libbrecht, Helen C. Morrison, and Benjamin Faber. Measurements of snow crystal growth dynamics in a free-fall convection chamber. *arXiv*; (0811.2994), 2008.
- [14] K. G. Libbrecht and H. M. Arnold. Measurements of ice crystal growth rates in air at -5 c and -10 c. *arXiv*; (0912.2518), 2009.
- [15] K. G. Libbrecht and R. Bell. Chemical influences on ice crystal growth from vapor. *arXiv*; (1101.0127), 2011.

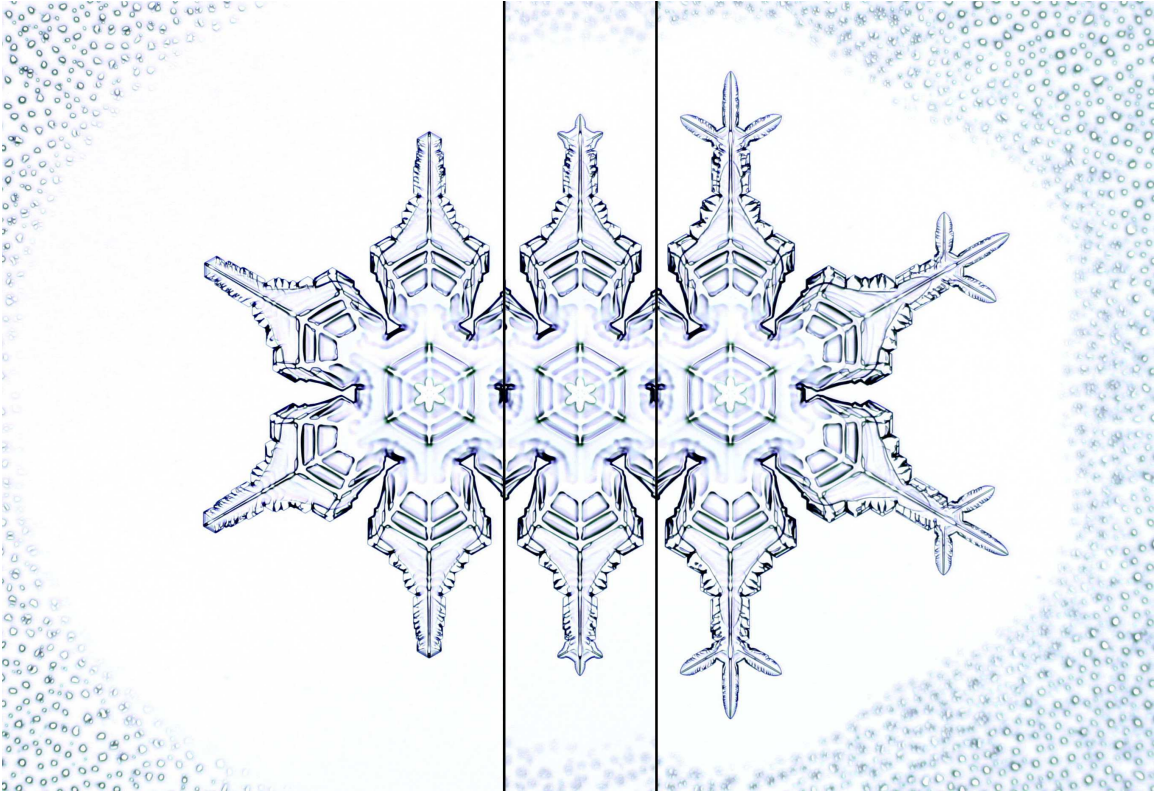


Figure 8: A composite image of a POP crystal taken at three different times, showing an induced sidebranching event. In the first image (left), the supersaturation was relatively low, which caused the tips of the branches to slow their growth and become faceted. In the second image, the supersaturation was increased, so water droplets condensed more closely around the outer edges of the crystal. The increased water supply caused sidebranches to sprout from the corners of the arm tips. In the third image, the sidebranches have grown longer while the supersaturation remained high. Note the symmetrical growth of the crystal, and that the tips of the branches and sidebranches remain rounded when the supersaturation is relatively high. Note also that most of the crystal growth takes place at the outermost edges of the crystal.



Figure 9: A dendritic POP crystal measuring 3.6 mm from tip to tip. After forming the inner part of the crystal, five sets of sidebranches were induced at regular intervals on the six outer branches. Natural snow crystals rarely show this degree of symmetry in their sidebranches.